

TWO-DIMENSIONAL PARAUNITARY COSINE MODULATED PERFECT RECONSTRUCTION FILTER BANKS[†]

Yuan-Pei Lin and P. P. Vaidyanathan

Dept. of Electrical Engineering, 116-81
California Institute of Technology
Pasadena, CA 91125.

Abstract

In this paper, we construct two-dimensional (2D) FIR paraunitary Cosine Modulated Filter Banks (CMFB). All the analysis and synthesis filters are cosine-modulated versions of a 2D non-separable prototype; each filter consists of two shifts of the prototype. The design of the filter bank involves only the optimization of the prototype. Furthermore, the complexity of the 2D filter bank is that of the prototype plus two non-separable DCT matrices.

1. Introduction

Recently, there has been considerable interest in the design of 2D filter banks. In [1], perfect reconstruction is achieved for a 2D two-channel FIR filter bank with diamond-shaped filters. Also in [2], transformations are used to design higher dimensional filter banks from filter banks of lower dimensions. Very recently, other authors have considered the same design problem, [3] [4].

In the context of one-dimensional (1D) filter bank design, the cosine modulated system is well-known for its low complexity and low design cost (see references in [5]). The design of the whole filter bank is reduced to the optimization of a prototype filter. The complexity of the analysis bank is equal to that of a prototype filter, plus a DCT matrix.

In this paper, we construct 2D FIR paraunitary cosine modulated filter banks. First we choose the analysis and synthesis filters such that major aliasing error is canceled and then we constrain the polyphase components of a prototype filter to achieve paraunitariness, hence perfect reconstruction. In the 2D CMFB, the analysis and synthesis filters are obtained by cosine modulating a 2D non-separable prototype. We only need to optimize the prototype filter to be a lowpass filter with a parallelogram support. The complexity of the analysis bank is that of the 2D prototype plus two non-separable DCT matrices. Design example will be given to demonstrate the idea.

Notations. The notations in this paper are as in [5]. Some notations are listed below.

1. *Unimodular matrix:* An integer matrix \mathbf{U} is unimodular if $|\det(\mathbf{U})| = 1$.
2. *The $\mathcal{N}(\mathbf{M})$ notation:* Let \mathbf{M} be a nonsingular

integer matrix. The notation $\mathcal{N}(\mathbf{M})$ is defined as the set containing integer vectors of the form

$$\mathbf{n} = \mathbf{M}\mathbf{x}, \mathbf{x} \in [0, 1)^D.$$

The number of elements in $\mathcal{N}(\mathbf{M})$ is denoted by $J(\mathbf{M})$, which is equal to $|\det(\mathbf{M})|$.

3. *Division theorem for integer vectors:* An integer vector \mathbf{n} has a unique representation with respect to an integer matrix \mathbf{M} , $\mathbf{n} = \mathbf{n}_0 + \mathbf{M}\mathbf{k}$, $\mathbf{n}_0 \in \mathcal{N}(\mathbf{M})$. This relation is denoted by $\mathbf{n} = \mathbf{n}_0 \bmod \mathbf{M}$.
4. *Lattice and quincunx lattice:* The lattice of a matrix \mathbf{M} is denoted by $LAT(\mathbf{M})$. The lattice of a 2×2 matrix \mathbf{M} is called quincunx if $\mathbf{M} = \begin{pmatrix} 1 & 1 \\ -1 & 1 \end{pmatrix} \mathbf{W}$, for some unimodular \mathbf{W} .
5. The symmetric parallelepiped $SPD(\mathbf{M})$ is the set

$$SPD(\mathbf{M}) = \{\mathbf{M}\mathbf{x}, \mathbf{x} \in [-1, 1)^2\}.$$

II. Construction of the 2D FIR paraunitary CMFB

In this section, we formulate the individual filters for the 2D CMFB based on the experience we have with 1D CMFB. Then we proceed to study the 2D filter bank from the consideration of alias suppression and cancelation.

2.1 Construction of the 2D CMFB from the analogy of 1D CMFB

Recall in a 1D M -channel CMFB, we start from a lowpass prototype with bandwidth π/M , which is half the bandwidth of a filter in a typical M -channel system. The prototype is then shifted by multiples of π/M . The shifted versions of the prototype are paired to obtain analysis filters. The resulting analysis filters have real coefficients and passband width $2\pi/M$. If the prototype is an ideal filter, those $2M$ shifts constitute a complete tiling for the interval $[0, 2\pi)$.

Consider the $J(\mathbf{M})$ -channel 2D filter bank, Fig. 2.1, with decimation matrix \mathbf{M} . Suppose \mathbf{M} is diagonalized as $\mathbf{M} = \mathbf{U}\mathbf{\Lambda}\mathbf{W}$, where \mathbf{U} and \mathbf{W} are unimodular and $\mathbf{\Lambda}$ is a diagonal matrix with diagonal entries $[\mathbf{\Lambda}]_{00} = \lambda_0$ and $[\mathbf{\Lambda}]_{11} = \lambda_1$. To emulate the 1D case, we begin from a prototype $P(\omega)$ with $SPD(\pi\mathbf{N}^{-T})$. The new matrix \mathbf{N} is given by

$$\mathbf{N} = \mathbf{M}\mathbf{W}^{-1} \underbrace{\begin{pmatrix} 1 & 0 \\ 0 & 2 \end{pmatrix}}_{\mathbf{L}} \mathbf{V}, \quad (1)$$

[†] Work supported in parts by NSF grant MIP 92-15785, Tektronix, Inc., and Rockwell International.

where \mathbf{V} is unimodular. Clearly, $J(\mathbf{N}) = 2J(\mathbf{M})$.

Let $\{\mathbf{k}_m, m = 0, 1, \dots, 2J(\mathbf{M}) - 1\} = \mathcal{N}(\mathbf{N})$ and let

$$Q_m(\omega) = P(\omega - 2\pi\mathbf{N}^{-T}(\mathbf{k}_m + \mathbf{b})), 0 \leq m < 2J(\mathbf{M}),$$

where \mathbf{b} can be $(0.5 \ 0)^T$ or $(0 \ 0.5)^T$. The whole frequency domain is tiled by the spectral support of $Q_m(\omega)$ for either choice of \mathbf{b} .

The next step is to choose m and m' such that $\mathbf{k}_{m'} = -\mathbf{k}_m - 2\mathbf{b} \bmod \mathbf{N}^T$. Then the impulse response of $Q_{m'}(\omega)$ is the conjugate of that of $Q_m(\omega)$. Combining $Q_m(\omega)$ and $Q_{m'}(\omega)$, we get $J(\mathbf{M})$ real-coefficient analysis filters.

$$\begin{aligned} H_m(\omega) &= Q_m(\omega) + Q_{m'}(\omega), \\ F_m(\omega) &= Q_m^*(\omega) + Q_{m'}^*(\omega), \end{aligned} \quad m = 0, 1, \dots, J(\mathbf{M}) - 1. \quad (2)$$

We have chosen $F_m(\omega) = H_m^*(\omega)$ in the above formulation as the system is paraunitary. The impulse response of the synthesis filter $f_m(\mathbf{n})$ and the impulse response of the analysis filters $h_m(\mathbf{n})$ are related by $f_m(\mathbf{n}) = h_m(-\mathbf{n})$. To make the idea of this construction more clear, we look at an example.

Example 2.1. Let

$$\mathbf{M} = \begin{pmatrix} 7 & -2 \\ 0 & 1 \end{pmatrix}, \mathbf{L} = \begin{pmatrix} 1 & 1 \\ 2 & 4 \end{pmatrix} \text{ and } \mathbf{b} = \begin{pmatrix} 0 \\ 0.5 \end{pmatrix}.$$

Then $J(\mathbf{M}) = 7$ and $\mathbf{N} = \begin{pmatrix} 3 & -1 \\ 2 & 4 \end{pmatrix}$. The prototype $P(\omega)$ has spectral support $SPD(\pi\mathbf{N}^{-T})$, Fig. 2.2(a). Fig 2.2(b) shows the shifts of $P(\omega)$ and spectral supports of the seven analysis filters $H_m(\omega)$.

It is noteworthy that a 2D separable CMFB obtained from 1D CMFB has four shifted copies of a separable 2D prototype. The preceding scheme is fundamentally different as each individual filter has only two shifted copies of a non-separable 2D prototype.

2.2 Alias suppression

Consider the m th subband. Due to decimation followed by expansion, both $Q_m(\omega)$ and $Q_{m'}(\omega)$ have $J(\mathbf{M})$ images. Since every filter has real coefficients, it is sufficient to inspect the overlapping between the images of $Q_m(\omega)$ and $F_m(\omega)$.

The output of $H_m(\omega)$ is decimated by \mathbf{M} and then expanded by \mathbf{M} . The images of $Q_m(\omega)$ are $Q_m(\omega - 2\pi\mathbf{M}^{-T}\mathbf{m})$, $\mathbf{m} \in \mathcal{N}(\mathbf{M}^T)$. Since $2\pi\mathbf{M}^{-T}\mathbf{m} = 2\pi\mathbf{N}^{-T}\mathbf{L}^T\mathbf{m}$, the images of $Q_m(\omega)$ are still confined to the grid of $Q_i(\omega)$, $i = 0, 1, \dots, J(\mathbf{N}) - 1$.

As $F_m(\omega)$ consist of $Q_m^*(\omega)$ and $Q_{m'}^*(\omega)$, we will look at the overlapping between $Q_m(\omega)$ and the two parts of $F_m(\omega)$ separately. Referring to Fig. 2.3, if

one image copy of $Q_m(\omega)$ is at any one of the shaded areas, there will be leakage of this image copy at the synthesis bank. Those shaded areas correspond to the shifts of $Q_m(\omega)$ by $2\pi\mathbf{N}^{-T}\mathbf{k}$, where $\mathbf{k} \in AS$ with AS defined as

$$AS \triangleq \left\{ \begin{pmatrix} 1 \\ 0 \end{pmatrix}, \begin{pmatrix} -1 \\ 0 \end{pmatrix}, \begin{pmatrix} 0 \\ 1 \end{pmatrix}, \begin{pmatrix} 0 \\ -1 \end{pmatrix} \right\}.$$

Recall that images of $Q_m(\omega)$ are shifts of $Q_m(\omega)$ by $2\pi\mathbf{N}^{-T}\mathbf{L}^T\mathbf{m}$. So if $LAT(\mathbf{L}^T)$ is quincunx, then $\mathbf{L}^T\mathbf{m} \notin AS$ and none of the images of $Q_m(\omega)$ will fall on top of the shaded areas.

Under the constraint that $LAT(\mathbf{L}^T)$ is quincunx, we can verify that $Q_{m'}^*(\omega)$ will be surrounded by images of $Q_m(\omega)$. Let $m = 1$ in Fig. 2.4, then Fig. 2.4 shows the situation in the first subband in Example 2.1. The four shaded areas are the images of $Q_1(\omega)$. Some leakage of those four image copies is inevitable and alias cancelation at the synthesis bank is required.

An additional result of constraining $LAT(\mathbf{L}^T)$ to be quincunx is that every $Q_m(\omega)$ has complex coefficients. This means all analysis filters have the same height.

2.3 Alias cancelation

Let $p(\mathbf{n})$ be the impulse response of the prototype $P(\omega)$. Suppose the prototype has linear phase with

$$p(\mathbf{n}) = p(\mathbf{n}_s - \mathbf{n}), \text{ for some integer vector } \mathbf{n}_s. \quad (3)$$

From previous study, we know $Q_1^*(\omega)$ overlaps with four images of $Q_1(\omega)$. Those images are labeled A , B , C and D in Fig. 2.4. Let us zoom in the discussion for the aliasing error due to image A . Image A is at the spectral support of $Q_0(\omega)$. But in the 0th subband, $Q_0^*(\omega)$ also overlaps with one particular image of $Q_0(\omega)$, which is at $Q_1(\omega)$. It can shown that these two aliasing errors cancel each other if

$$\mathbf{n}_s = 0.5\mathbf{N} \begin{pmatrix} 1 \\ 1 \end{pmatrix} \bmod \mathbf{N}. \quad (4)$$

Cancelation of aliasing error due to images B , C and D is similar. This reasoning of alias cancelation can be applied to every other subband. However, it is necessary that $\mathbf{N}(0.5 \ 0.5)^T$ be an integer vector. This property is guaranteed if $LAT(\mathbf{L}^T)$ is quincunx: when $LAT(\mathbf{L}^T)$ is quincunx, we can write $\mathbf{L} = \mathbf{W}_L \begin{pmatrix} 1 & 1 \\ -1 & 1 \end{pmatrix}$, for some unimodular \mathbf{W}_L . So $\mathbf{N}(0.5 \ 0.5)^T$ is always an integer vector.

Summarizing, we have formulated the analysis and synthesis filters in the 2D CMFB. We have also studied the conditions for cancelation of major aliasing error. The conditions are 1) $LAT(\mathbf{L}^T)$ is quincunx and 2) \mathbf{n}_s is as in (4). In the next section, we start from the

construction in Sec. II and find out the conditions for perfect reconstruction of the 2D CMFB.

III. The 2D paraunitary FIR CMFB

In this section, we provide the conditions under which the polyphase matrix is paraunitary and the 2D CMFB has perfect reconstruction. Let $\{\mathbf{n}_i, i = 0, 1, \dots, 2J(\mathbf{M}) - 1\} = \mathcal{N}(\mathbf{N}\mathbf{V}^{-1})$ and let $G_i(\omega)$ be the type 1 polyphase component of the prototype with respect to $\mathbf{n}_i \in \mathcal{N}(\mathbf{N}\mathbf{V}^{-1})$, then

$$P(\omega) = \sum_{i=0}^{2J(\mathbf{M})-1} G_i(\mathbf{N}^T\omega) \exp(-j\omega^T \mathbf{n}_i) \quad (5)$$

Notice that we use index $\mathbf{n} \in \mathcal{N}(\mathbf{N}\mathbf{V}^{-1})$ rather than $\mathbf{n} \in \mathcal{N}(\mathbf{N})$.

When $P(\omega)$ has linear phase as in (3) and \mathbf{n}_s is as in (4), the polyphase components are pairwise related. In particular, the i th and \hat{i} th polyphase components are related, where \hat{i} is such that $\mathbf{n}_{\hat{i}} = \mathbf{U} \begin{pmatrix} 0 & \lambda_1 \\ \lambda_1 & 0 \end{pmatrix}^T \mathbf{n}_i$. Let $g_i(\mathbf{n})$ and $g_{\hat{i}}(\mathbf{n})$ be the impulse responses of $G_i(\omega)$ and $G_{\hat{i}}(\omega)$, then

$$g_{\hat{i}}(\mathbf{n}) = g_i(-\mathbf{n} - \mathbf{d}_i), \quad (6)$$

for some integer vector \mathbf{d}_i .

Theorem 3.1. Consider the filter bank in Fig. 2.1 and the choice of analysis and synthesis filters in (2). Let the matrix \mathbf{N} be as given in (1), where $LAT(\mathbf{L}^T)$ is quincunx. Also let the prototype be linear-phase and \mathbf{n}_s , given in (3), satisfy (4). Then the CMFB in Fig. 2.1 is paraunitary (i.e., the polyphase matrix is paraunitary) if and only if

$$G_i^*(\omega)G_i(\omega) + G_{\hat{i}}^*(\omega)G_{\hat{i}}(\omega) = c,$$

where c is some constant and $\mathbf{n}_{\hat{i}} = \mathbf{n}_i + \mathbf{U} \begin{pmatrix} 0 \\ \lambda_1 \end{pmatrix}$.

A proof of this theorem can be found in [6].

IV. Efficient implementation of the 2D CMFB

Using the polyphase representation of the prototype in (5), the analysis filters in (2) can be rewritten as

$$H_m(\omega) = \sum_{i=0}^{2J(\mathbf{M})-1} 2G_i(\mathbf{N}^T\omega - 2\pi\mathbf{b}) [\mathbf{C}]_{mi} \exp(-j\omega^T \mathbf{n}_i),$$

where $[\mathbf{C}]_{mi} = \cos(2\pi(\mathbf{k}_m + \mathbf{b})^T \mathbf{N}^{-1} \mathbf{n}_i)$,

$m = 0, 1, \dots, J(\mathbf{M}) - 1, i = 0, 1, \dots, 2J(\mathbf{M}) - 1$.

The above expression for the analysis filters gives rise to the efficient implementation in Fig. 4.1. The computation of \mathbf{C} is equivalent to the computation

of two 2D non-separable DCT matrices. The figure demonstrates that the complexity of the 2D CMFB is that of the prototype plus two 2D non-separable DCT matrices.

V. Design example

Example 5.1. We continue on Example 2.1. Fig. 5.1(a) shows the pairs of polyphase components that are power complementary and Fig. 5.1(b) shows the pairs of polyphase components that are related in pairs as in (6), due to linear phase property of $P(\omega)$. In the figures, we use the notation $\mathbf{E}_{n_1}^{n_0}$ to denote the polyphase component \mathbf{E}_i with respect to $\mathbf{n}_i = \mathbf{U} \begin{pmatrix} n_0 & n_1 \\ n_1 & 0 \end{pmatrix}^T, n_0 = 0, 1, \dots, \lambda_0, n_1 = 0, 1, \dots, 2\lambda_1 - 1$. Notice that \mathbf{E}_0^0 and \mathbf{E}_1^0 are power complementary and are also related because of linear phase of $P(\omega)$. As a result, these two polyphase components are merely a delay. When \mathbf{E}_0^i and $\mathbf{E}_1^i, i = 1, 2, 3$, are power complementary, \mathbf{E}_0^i and $\mathbf{E}_1^i, i = 4, 5, 6$, will also be power complementary because $P(\omega)$ is linear-phase. We can optimize $P(\omega)$ subject to only the condition that \mathbf{E}_0^i and $\mathbf{E}_1^i, i = 1, 2, 3$, are power complementary. This condition can be satisfied by using the 2D paraunitary lattice, [7].

Fig. 5.2 shows the support of impulse response of the prototype filter, $p(n_0, n_1)$. The support of $p(n_0, n_1)$ resembles the shape of $SPD(2\mathbf{N})$. The corresponding frequency response of the prototype is shown in Fig. 5.3. The stopband attenuation of the prototype is 17 dB. In this optimization, each of the fourteen polyphase components has four coefficients.

Reference

- [1] R. Ansari and C. Guillemot, "Exact reconstruction filter banks using diamond FIR filters," Proc. Int. Conf. on new trends in Comm. Control, and Signal Proc., Turkey, July 1990.
- [2] I. A. Shah and A. A. C. Kalker, "Generalized theory of multidimensional M-band filter bank design," SP VI: Theories and Applications, 1992.
- [3] M. Ikehara, "Cosine-modulated 2 dimensional FIR filter banks satisfying perfect reconstruction," Proc. ICASSP, April 1994.
- [4] S. C. Chan, "Two dimensional nonseparable modulated filter banks," Proc. ICASSP, April 1994.
- [5] P. P. Vaidyanathan, *Multirate systems and filter banks*, Englewood Cliffs, Prentice Hall, 1993.
- [6] Y.-P. Lin and P. P. Vaidyanathan, "Study of 2D cosine modulated filter banks," (In preparation).
- [7] V. C. Liu and P. P. Vaidyanathan, "On factorization of subclass of 2D digital FIR lossless matrices for 2D QMF bank application," *IEEE Trans. CAS*, June 1990.

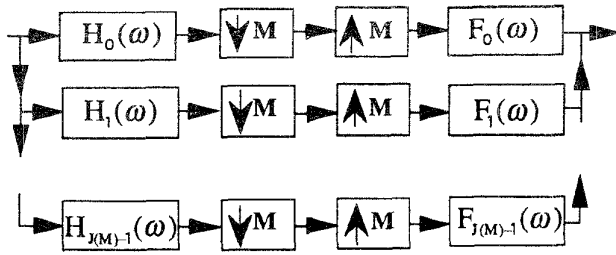


Fig. 2.1. $J(M)$ channel maximally decimated filter bank.

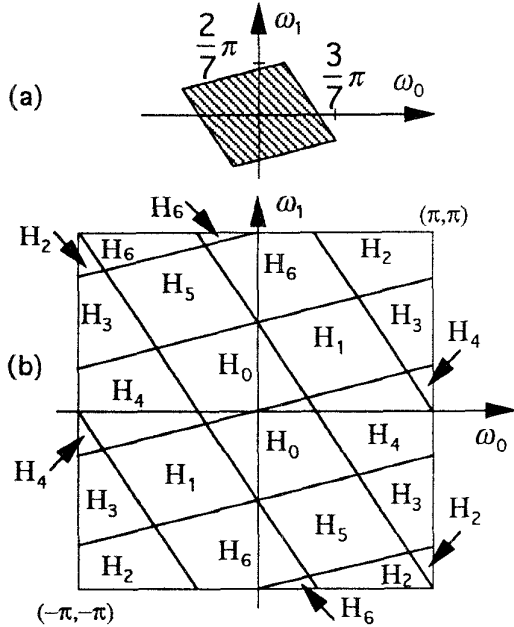


Fig. 2.2. Example 2.1. (a) Spectral support of the prototype $P(\omega)$, $SPD(\pi N^{-T})$. (b) Spectral support of the analysis filters.

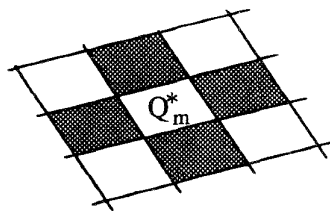


Fig. 2.3. Pertaining to alias suppression.

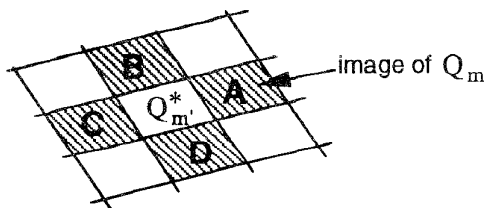


Fig. 2.4. Illustration of overlapping between Q_m^* and the images of Q_m .

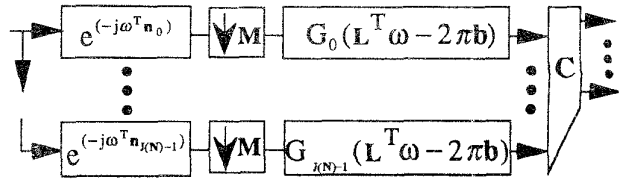


Fig. 4.1. Efficient implementation of the analysis bank of the 2D cosine modulated filter bank.

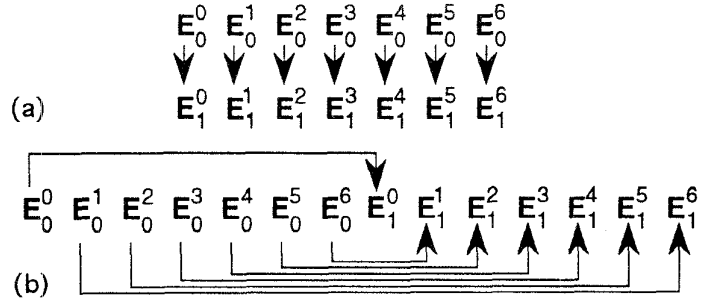


Fig. 5.1(a) Polyphase components of $P(\omega)$ that are pairwise power complementary. (b) Polyphase components of $P(\omega)$ that are related due to linear phase of $P(\omega)$.

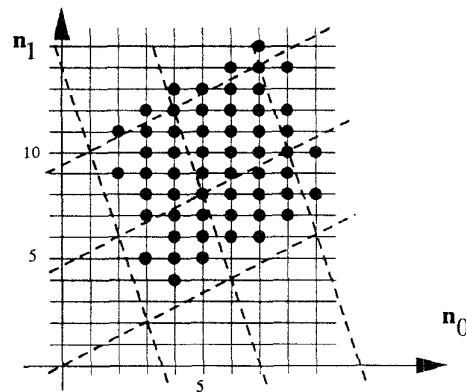


Fig. 5.2. Impulse response support of the prototype. Intersection points of the dashed lines are on the lattice of N . Solid lines represent integers.

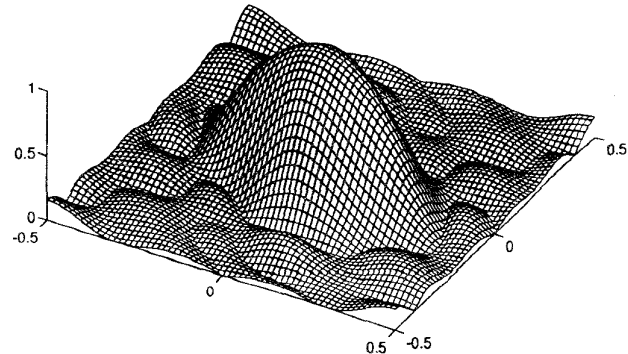


Fig. 5.3. Example 5.1. Magnitude response of the prototype with frequency normalized by 2π .